DOI: 10.1002/ejic.200700436

Combined Studies on the Surface Coordination Chemistry of Benzotriazole at the Copper Electrode by Direct Electrochemical Synthesis and Surface-Enhanced Raman Spectroscopy

Ya-Xian Yuan,[a] Ping-Jie Wei,[a] Wei Qin,[a] Yong Zhang,[a] Jian-Lin Yao,*[a] and Ren-Ao Gu[a]

Keywords: Benzotriazoles / Copper / Surface coordination / Electrochemistry / Raman spectroscopy

The surface coordination chemistry of benzotriazole (BTAH) on a Cu electrode was investigated by electrochemical synthesis of surface complexes and in situ electrochemical surface-enhanced Raman spectroscopy (SERS) in nonaqueous solution. Two different surface complexes were prepared in solution with or without triphenylphosphane (PPh_3). A new mixed-valence Cu–N cluster compound containing BTAH was synthesized by direct electrochemical oxidation of Cu in nonaqueous solutions with PPh_3. The final product, $Cu_5Cl(BTA)_5(PPh_3)_4$ was crystallized and characterized by microanalysis and Raman spectroscopy together with X-ray crystallographic determinations. The complex crystallized in a monoclinic space group ($P2_1/n$) with lattice parameters a = 16.739(2) Å, b = 18.919(2) Å, c = 31.042(4) Å, β = 103.194(3)°, V = 9571.0(19) Å^3, R_1 = 0.0704, wR_2 = 0.1643. The results showed that the complex was a pentanuclear compound. The central Cu^{II} atom is coordinated to four equatorial and one axial BTA^- ligands to form a distorted tetragonal pyramidal coordination polyhedron, whereas each surrounding Cu^I ion is in a distorted tetrahedral environment. The in situ SERS studies revealed that the BTA^- ion was coordinated to a Cu surface through its two N atoms of the triazole ring to form a surface polymer complex of $[Cu(BTA)]_n$, which suppressed the dissolution and oxidation of Cu effectively. The introduction of PPh_3 blocked the surface coordination of BTAH with the electrode, and a complex of BTA^- and PPh_3 with Cu was formed in the bulk solution.

Introduction

The coordination chemistry of metal surfaces exposed to a corrosion medium has attracted considerable attention from the coordination chemists and surface scientists because of its economic importance.[1–5] For example, some organic molecules adsorbed on particular metal surfaces form a compact complex layer that can inhibit the corrosion of the surface effectively.[6–12] Despite the importance of special organic inhibitors, little attention has been paid to the investigation of how they bind or coordinate to the metal surfaces or as to why seemingly minor modifications in the structures of the active organic compounds can have a profound effect on their efficiency. Therefore, investigation into the interaction or the coordination chemistry of organic ligands with metal surfaces could be beneficial to obtain deeper insight into the adsorption behavior of ligands and their relevant surface coordination processes.

Generally, the deduction of the surface reaction mechanisms that include strong chemisorption or the formation of films (surface complexes) should be based on the known habits of the components and the structures of the surface complexes. One reliable and direct way to obtain such components is by the preparation of the corresponding surface complexes under conditions similar to those of the electrode surface. So far, many methods have been used to synthesize the relevant surface complexes. For example, the soluble metal salt and the ligands can simply be mixed in aqueous/nonaqueous solutions to produce the corresponding complexes, or the metal salt and the ligand solid powders can be mixed to form the complexes, a so-called solid-phase synthesis.[13] However, the direct electrochemical synthesis performed for the first time by Tuck and coworkers has exhibited several advantages for providing the comparable conditions of the surface.[14–21] This method consists in oxidizing a sacrificial metal anode in the nonaqueous solution with one or more appropriate kinds of ligands. Therefore, the synthetic conditions, including the bulk metal electrode, applied potential/current, solution (aqueous or nonaqueous), and electrolyte resemble the real electrode reaction system. As a consequence, on the basis of the interactions and chemical bonding between the ligand and the metal, it is reasonable to deduce the surface adsorption processes with the participation of some ligands on the electrode in the complex prepared by the electrochemical synthetic

[a] Department of Chemistry, Suzhou University (Dushu Lake campus),
Suzhou 215123, China
Fax: +86-512-65880089
E-mail: jlyao@suda.edu.cn

method. Moreover, no oxidant or reductant is introduced into the system of the electrochemical synthesis, and this avoids the possible complicated processes resulting from redox reactions. Alternatively, the oxidation of the metal electrode and the reduction of the ligands were carried out by the "clean" electron, which was removed or added on the anode and cathode by the applied potential/current. This dramatically decreased the contamination due to extraneous chemicals not only in the reaction processes but also in the separation of the final products. Most importantly, the adjustable applied potential/current made the reaction become highly selective, and thus enabled us to obtain the expected final products. However, the introduction of supporting electrolytes might be found in the final product in the form of anions or cations. In low concentrations, the appropriate amount of supporting electrolyte can, to some extent, minimize its negative effect on the complexes. Therefore, the direct electrochemical synthetic technique provided an effective way to simulate the electrochemical adsorption and reaction on the electrode surface, which allowed the structure and composition of the surface species to be obtained.

However, information on the dynamic and mechanistic aspects of the surface processes was not obtained by the above-mentioned techniques. Information about the processes that occur on the electrode surface can be gained by several modern surface techniques, such as scanning tunneling microscopy (STM), X-ray photoelectron spectroscopy (XPS), electron energy loss spectroscopy (EELS), sum frequency generation (SFG), and infrared and Raman spectroscopy.[10,11,22–25] Among them, Raman spectroscopy is a powerful tool for the investigation of the surface chemistry of adsorbed molecules involving adsorption and coordination at the liquid–solid interface, provided that the surface Raman signals are sufficiently enhanced.[26,27] In particular, surface-enhanced Raman scattering (SERS) has been shown to be a good method for determining the structure of molecules adsorbed on electrode surfaces.[28–34] Furthermore, unlike EELS and XPS, SERS can yield detailed surface information free from the interference of the bulk phase even at metal–liquid interfaces, and it has been widely used to investigate the dynamic and mechanisms of surface processes in situ.

To date, most coatings for metals have contained corrosion inhibitors as key constituents, and their activity was dependent on the surface coordination chemistry of the inhibitor. Benzotriazole (BTAH) is one of the most effective inhibitors for Cu and its alloys. Since the pioneering work of Cotton and coworkers,[35] the adsorption/coordination behavior and bonding structure between BTAH and a Cu substrate have been extensively studied by many authors by using various techniques, including electrochemical, surface analytical, and spectroscopic techniques.[36–40] Most of the previous work revealed that BTAH inhibited the corrosion of Cu in a wide pH range and potential region. For example, in different potential regions, BTAH can form a chemisorbed layer or a multilayer polymerized structural film with a larger thickness that increases the inhibition of corrosion significantly. The details of the mechanism by which the film forms and protects the metal are the subject of much investigation and debate.

Therefore, a powerful in situ technique with high surface sensitivity that is able to provide specific molecular information on metal surfaces has long been desired. Many researchers reported studies on the inhibition effect of BTAH by electrochemical SERS in aqueous solutions. To the best of our knowledge, there is no report on the studies of the adsorption/coordination chemistry and film formation of inhibitors in nonaqueous solutions. However, nonaqueous solvents are extremely important in both pure and applied electrochemistry, particularly as a component of the electrolyte that is in contact with the electrodes. Moreover, the involved organic molecules or inorganic ions can exhibit different inhibition efficiencies.[40,41] For example, the introduction of I^- ions into solutions containing BTAH makes the inhibition efficiency for both the anodic and cathodic processes become even more remarkable,[42,43] which thus indicates the existence of a synergetic effect between the I^- ions and benzotriazole on the inhibition. However, some organic ligands might play a negative role in the inhibition when it coexists with BTAH. For example, the introduction of ligands such as β-diketonate, acetylacetone, and triphenylphosphane (PPh_3) can result in remarkable differences in the structures of metal complexes with BTAH, specifically, the transformation of single metal nuclear to multinuclear complexes.[1,44–49] Therefore, it is worth investigating the inhibition of BTAH in nonaqueous solutions containing some organic molecules that might play an important role in the formation of surface complex films. In contrast, it is highly desirable to extend SERS studies directly to wider applications in surface science, not only for the various processes of corrosion and inhibition, but also for the surface coordination chemistry of BTAH together with other ligands. Triphenylphosphane is one of the most commonly used ligands in organometallic and coordination chemistry, and it is one of the most common ligands found in homogeneous transition-metal catalysts for the binding and transformation of organic substrates.[50–53] Phosphanes in general have been mainly used as protecting groups in organic synthesis as well as in catalytic processes, in which they were responsible for the decisive reaction step.[54] For this reason, PPh_3 was chosen as the second metal-binding domain in studying the surface coordination chemistry of BTAH on a Cu electrode.

In the present work, the adsorption behavior and film formation of BTAH were investigated by in situ electrochemical SERS on the surface of a Cu electrode in nonaqueous solution and by the coordination chemistry between the Cu surface and BTAH with and without PPh_3. Meanwhile, for the determination of the compositions and structures of the surface complexes, two kinds of complexes of BTAH and Cu with and without PPh_3 were synthesized by direct electrochemical synthesis and characterized by microanalysis, X-ray crystallographic measurements, and Raman spectroscopy. The modes of inhibitor on the Cu surface in nonaqueous solution were proposed.

Results and Discussion

Electrochemical Synthesis of the Complex

The electrochemical oxidation of Cu provided a convenient route to its coordination compound with the title ligands in a "one pot" procedure. One of the advantages of these techniques is that the metal in the product is frequently in a low oxidation state as the starting point is the element itself. It should be noted that the deposited layer on the anode resulted in its low conductivity. Thus, a mild voltage was applied to the system to maintain electrolysis. However, the electrochemical reaction potential was less than the applied voltage and the current density was maintained with a small value of about 5–8 $mA\,cm^{-2}$ during the electrolytic procedures. Therefore, the conditions used in the direct electrochemical synthesis were comparable to those at the Cu electrode surface, which was studied by in situ SERS. Complexes 1 and 2, which were synthesized by the electrochemical method, were expected to have the same composition as the Cu electrode surface in the electrochemical system for the in situ SERS investigation.

The stoichiometry of the electrochemical reaction is indicated by the electrochemical efficiency outlined in Equations (1) and (2), where m is the weight lost at the Cu anode, M is the molar mass of Cu, z is the valence of the Cu ion, i is the applied current, t is the electrolysis time, and F is Faraday constant; the value $\int_t^0 idt$ is determined by the silver coulomb meter, which is linked into the circuit, and is defined as the number of moles of metal dissolved from the anode per Faraday of charge. In the present study, the value of E_f of $0.99\,mol\,F^{-1}$ and $0.98\,mol\,F^{-1}$ implied that the monovalent Cu^I complex was formed on the electrode surface at the initial stage in solutions without/with PPh_3, respectively. The electrochemical systems can be represented as Pt(–)|CH_3CN, BTAH, electrolyte|Cu(+) and Pt(–)|CH_3CN, PPh_3, BTAH, electrolyte|Cu(+), respectively. The electrode reactions are outlined in Equations (3) and (4).

$$E_f = (m/M)F/\int_0 \mathrm{idt}(\mathrm{mol}/F) \quad (1)$$

$$z = 1/E_f = M\int_0^t \mathrm{idt}/mF \quad (2)$$

$$\text{cathode: } BTAH + e \rightarrow BTA^- + 1/2H_2 \quad (3)$$

$$\text{anode: } Cu \rightarrow Cu^+ + e \quad (4)$$

For the solution without PPh_3, the BTA^- anion coordinated to the Cu^+ ion immediately to form a compact film that attached itself to the electrode surface. Actually, at the initial stage of the electrochemical synthesis, to be exact, as soon as the electrolytic current was applied, a yellow precipitate was produced that attached itself to the Cu electrode surface. At last, a dark yellow product was obtained after separation of the precipitate from the solution. Unfortunately, no crystal of the final product was obtained because of its poor solubility in most solvents. Elemental microanalysis of the sample gave a composition of C 61.35, H 4.18, N 11.47 (CuBTA: calcd. C 59.74, H 4.15, N 10.55) and revealed that the molar ratio of Cu to the BTA^- anion was 1:1. Previous investigations of BTAH adsorbed on Cu electrodes showed that compact polymer films of $(CuBTA)_n$ were attached to the surface and inhibited the corrosion of Cu effectively in the aqueous solution;[12,29,40] this is in agreement with the synthesized sample that was prepared by mixing the Cu^+ compound with the BTAH solution. Therefore, it is reasonable to assume that the formula of the present sample was $(CuBTA)_n$ (complex 1). The overall reaction at the electrode surface is depicted in Equation (5). On the basis of previous experimental results, its structure was proposed as that shown in Figure 1.

$$nBTAH + nCu \xrightarrow{\text{electrolysis}} (CuBTA)_n + n/2H_2\uparrow \quad (5)$$

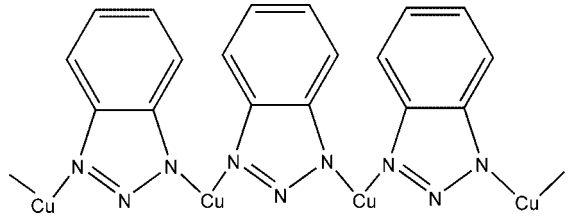

Figure 1. Proposed structure of the $(CuBTA)_n$ polymer complex.

The normal Raman spectrum of $(CuBTA)_n$ was presented with in situ SERS studies. The large blueshift of the triazole and benzene ring mode indicated the coordination of the BTA^- ion with Cu. The detailed structure information will be discussed in the next section.

After the addition of PPh_3, no precipitation was observed on the Cu electrode surface or in the solution at the initial stage of the electrolytic reaction. With an increase in the electrolysis time, a brown-yellow precipitate was formed at the bottom of the flask. The absence of precipitation at the beginning of the electrochemical synthesis in the CH_3CN solution with BTAH and PPh_3 indicated that no film was attached to the surface or that the prepared complex might be soluble in the CH_3CN solution (normally, with a low solubility). To separate the precipitate, the nonaqueous solution was transferred into the fridge and yellow crystals were formed. Both the BTA^- and PPh_3 signals were detected together in the normal Raman measurement of the crystal. The frequency of the triazole and benzene ring mode of BTA^- was shifted to 1031 cm^{-1}, which is an indication of the coordination of the BTA^- ion to the Cu electrode. This result revealed that both the BTA^- ion and the PPh_3 ligand coordinate to the Cu ion. The final molecular formula and structure of this crystal should be deduced from its X-ray crystal structure.

Crystal Structure of $Cu_5(BTA)_5(PPh_3)_4Cl$

Selected bond lengths and angles of the $Cu_5(BTA)_5(PPh_3)_4Cl$ complex are listed in Table 1. The $Cu_5(BTA)_5$-

$(PPh_3)_4Cl$ complex crystallizes as a pentanuclear complex, and its molecular structure is illustrated in Figure 2. Because the benzotriazolate ion has a charge of –1, the pentacopper complex is a mixed-valent material that contains four Cu^I ions and one Cu^{II} ion. The central Cu^{II} ion is surrounded by four tetrahedrally coordinated Cu^I ions held by bridging BTA^- ligands. In the title complex, each tridentate BTA^- ligand bridges two Cu^I ions in two sides and coordinates to the central Cu^{II} ion through its central nitrogen atom. The central Cu^{II} ion is coordinated to four equatorial and one axial BTA^- ligands at the N2, N5, N8, N11, and N14 positions, and it has a distorted tetragonal pyramidal coordination geometry with average distances of Cu^{II}–N_{eq} 2.050(1) Å and Cu^{II}–N_{ax} 2.294(3) Å. These values are comparable to the Cu^{II}–N bond lengths (2.08 and 2.29 Å, respectively) in the related $Cu_5(BTA)_6(tfpbd)_4$ complex (tfpdb = 4,4,4-trifluoro-1-phenyl-1,3-butanedione).[47] Each surrounding Cu^I ion is four-coordinate with two types of coordination environments. For example, Cu3 (or Cu4) is in a distorted tetrahedral (CuN_3P) environment and is bound to three nitrogen atoms from different BTA ligands and a phosphorus atom in PPh_3. The Cu^I–N lengths Cu3–N9, Cu3–N3, and Cu3–N13 are about 2.061 Å and are close to those values in the complex [CuL(PPh_3)] {L = bis(2-pyridyl)[2-(6-methoxy)pyridyl]methoxymethane} with the similar core of CuN_3P.[55] In addition to Cu1 (or Cu2) being coordinated to two nitrogen atoms in two different BTA^- ligands and a phosphorus atom in PPh_3, it is also coordinated to a chloride ion that bridges two Cu centers with a Cu···Cu separation of 4.822 Å. The average value of all Cu^I–P bond lengths (about 2.1766 Å) is a little shorter than the value in $[Cu_4(BTA)_3(PPh_3)_4][Cu(PPh_3)_3](BF_4)_2$ [2.200(5) Å],[49] whereas the Cu^I–Cl bond lengths [Cu1–Cl1 2.4456(13) Å, Cu2–Cl1 2.4619(13) Å] are close to the value of about 2.455(1) Å in the $Cu_2Cl_2(PPh_3)_3$ complex together with a bridging chloride ion.[56]

Table 1. Selected bond lengths and bond angles of the $Cu_5(BTA)_5(PPh_3)_4Cl$ complex.

Bond lengths [Å]			
Cu1–N1	2.041(3)	Cu3–N9	2.060(4)
Cu1–N4	2.067(3)	Cu3–N3	2.061(3)
Cu1–P1	2.1860(12)	Cu3–N13	2.062(4)
Cu1–Cl1	2.4456(13)	Cu3–P3	2.1813(12)
Cu2–N7	1.994(4)	Cu4–N15	2.031(4)
Cu2–N10	2.006(4)	Cu4–N6	2.081(3)
Cu2–P2	2.1435(15)	Cu4–N12	2.106(4)
Cu2–Cl1	2.4619(13)	Cu4–P4	2.1956(12)
Cu5–N2	2.033(3)	Cu5–N14	2.294(3)
Cu5–N11	2.050(3)	Cu5–N5	2.064(3)
Cu5–N8	2.052(4)		
Bond angles [°]			
N1–Cu1–N4	91.89(14)	N1–Cu1–Cl1	97.69(10)
N1–Cu1–P1	130.91(10)	N4–Cu1–Cl1	93.65(10)
N4–Cu1–P1	127.92(10)	P1–Cu1–Cl1	105.78(5)
N7–Cu2–N10	96.33(16)	N9–Cu3–P3	120.67(11)
N7–Cu2–P2	128.18(11)	N3–Cu3–P3	122.72(10)
N10–Cu2–P2	126.78(12)	N13–Cu3–P3	117.46(11)
N7–Cu2–Cl1	94.95(12)	N15–Cu4–N6	99.40(14)
N10–Cu2–Cl1	98.03(11)	N15–Cu4–N12	96.11(14)
P2–Cu2–Cl1	104.44(5)	N6–Cu4 –N12	93.10(13)
N9–Cu3–N3	94.06(14)	N15–Cu4–P4	124.37(10)
N9–Cu3–N13	98.83(15)	N6–Cu4–P4	119.86(10)
N3–Cu3–N13	97.63(14)	N12–Cu4–P4	117.44(10)
N2–Cu5–N11	175.34(14)	N2–Cu5–N5	90.64(13)
N2–Cu5–N8	88.28(14)	N11–Cu5–N5	88.39(13)
N11–Cu5–N8	92.08(14)	N8–Cu5–N5	172.31(14)
N2–Cu5–N14	94.02(13)	N5–Cu5–N14	93.49(12)
N11–Cu5–N14	90.59(13)	Cu1–Cl1–Cu2	158.56(6)
N8–Cu5–N14	94.17(13)		

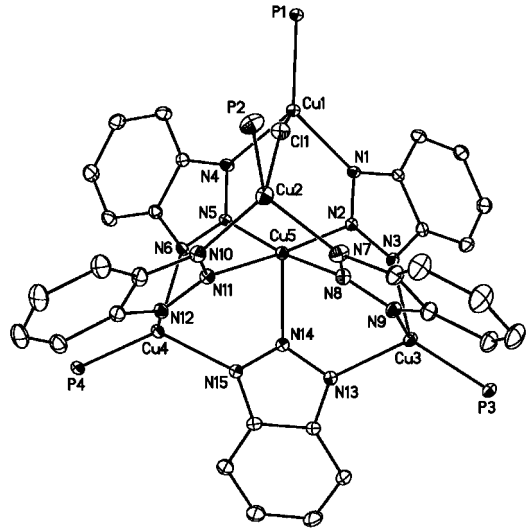

Figure 2. ORTEP drawing of the $Cu_5Cl(BTA)_5(PPh_3)_4$ complex. Hydrogen atoms are omitted for clarity.

For the Cu^I ion bridged by the axial benzotriazolate anion and the chloride ion, the average distance between the surrounding Cu^I ion is 5.315 Å and the distance increases to about 5.886 Å for the Cu^I ion bridged by the equatorial benzotriazolate anions, whereas the average distance of about 3.500 Å between the surrounding Cu^I and central Cu^{II} ions is much shorter than the above-mentioned value. The structure of the complex bears resemblance to that of $Cu_5(BTA)_6(t\text{-}C_4H_9NC)_4$,[44] where the latter contains an extra BTA^- group instead of the bridging chloride ion.

In Situ Electrochemical SERS Investigation

Figure 3 presents a set of potential-dependent SERS spectra of BTAH from a roughened Cu electrode in a wide potential range in acetonitrile solution with or without PPh_3 together with the normal Raman spectra of two complexes prepared by an electrochemical method for comparison. The series of spectra on the right side of Figure 3 unambiguously demonstrate the change in spectral features over a narrow range. Because the surface coordination of the BTA^- ion to the Cu electrode occurs in a positive potential range irreversibly, which was proven by relevant SERS studies in aqueous solution,[8,12] the potential-dependent spectra were recorded stepwise starting from a negative limit potential to more positive potentials so that all the ad-

sorption and surface coordination processes could be observed. It can be seen that the SERS spectra changed significantly with the applied potential not only in the intensity, but also in the frequency of the relevant bands. The spectra showed a similar spectral feature to that of the BTAH solid in the extremely negative potential region both in solution with or without PPh_3. For example, the surface spectra at –0.9 V without PPh_3 and at –1.0 V with PPh_3 exhibited the same frequency as the free BTAH for the triazole and benzene ring mode at 1022 cm^{-1}, respectively. This normally can serve as direct evidence for the determination of the coordination configuration of BTAH on the metal surface, although in this sample this band broadened significantly because of the complicated surface structure of the Cu electrode (as shown in Figure 3, right).[12] Our previous results indicated that the BTA^- ion of the surface complex film showed a blueshift to ca. 1040 cm^{-1} for this band. Therefore, the high similarity of the SERS spectra of BTAH on the surface to that from the bulk solution revealed the existence of an adsorption adlayer of BTAH molecules in the relative negative potential region in both solutions.

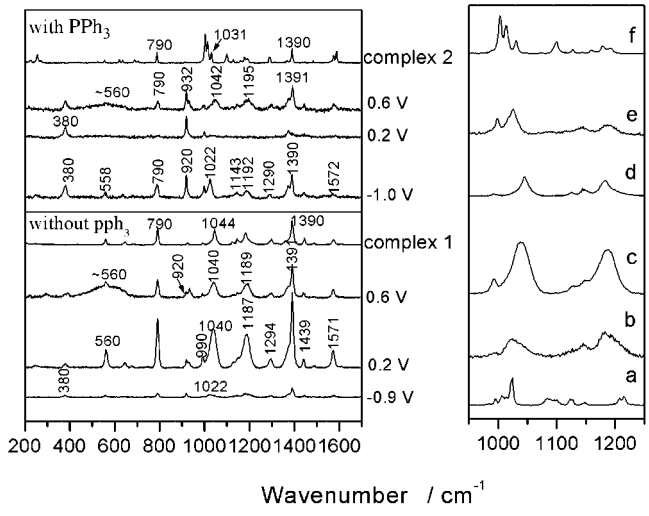

Figure 3. Potential dependent SERS spectra of BTAH adsorbed on the Cu electrode in acetonitrile solution without (bottom) and with 0.01 mol dm^{-3} PPh_3 (upper) together with the normal Raman spectra of two surface complexes (left). The figure presented on the right is for comparison in the range from 950 to 1250 cm^{-1}: (a) BTAH solid; (b) without PPh_3 at –0.9 V; (c) 0.2 V; (d) complex 1; (e) with PPh_3 at –1.0 V; and (f) complex 2.

By moving the potential positively, the signal intensity also increased greatly and the frequency of the triazole and benzene ring mode shifted to 1040 cm^{-1} at 0.2 V in the solution without PPh_3. Moreover, the surface spectrum at 0.2 V exhibited the same spectral features as that of the electrochemically synthesized $[Cu(BTA)]_n$ (complex 1; Figure 3, right). Most interestingly, the color of the electrode surface changed from brown to gray after the positive potential excursion, and the SERS measurement on the electrode in air without potential control exhibited similar spectral features to those in solution in the positive potential region. It was reported by many researchers that the BTA^- ion can adsorb onto the Cu surface to form an irreversible compact polymer film of $[Cu(BTA)]_n$, which increases the inhibition efficiency dramatically in a certain potential region in aqueous solutions.[8,9,12,35–37] Therefore, it is reasonable to assume that the observed surface Raman spectrum at 0.2 V comprised contributions from this irreversible polymer film attached to the Cu surface in a wide potential range, that is, the BTAH was adsorbed on the surface by the coordination of N atoms with Cu atoms. In the extremely positive potential region, the signal of the film decreased remarkably. This occurred mainly because of the following two reasons: (1) the disappearance of or decrease in the SERS activity of the Cu surface owing to the oxidation of the Cu surface and (2) the partial breakage of the polymer film due to the formation of Cu oxide. At 0.6 V, the intensities of the bands decreased and a broad band at ca. 560 cm^{-1} was detected with a sharp band at 560 cm^{-1}. The broad band was assigned to the stretching vibrational mode of Cu–O and the sharp band was assigned to the triazole ring torsion mode. Therefore, the observation of broad bands revealed the formation of Cu oxide in this potential region.

It is reasonable to assume that the surface complex (surface film) has the same composition as the synthesized complex. Therefore, on the basis of the fact that the potential-dependent adsorption behavior in nonaqueous solutions was similar to that in aqueous solutions, one can assume that BTAH adsorbs in the form of neutral BTAH molecules onto the Cu surface to form an adsorption layer in the negative potential region and in the form of BTA^- ions to form a compact polymer film of the type $[Cu(BTA)]_n$ in the positive potential region; the polymer film partially breaks in the most positive potential region. The formation of a surface complex film results in a more compact barrier layer, which leads to a higher inhibition effect. Most interestingly, when a small amount of PPh_3 (the same concentration as BTAH) was introduced into the solution as above and the same experimental processes were performed, significant spectral changes were found. For example, the Raman signal of BTA/BTAH was not detected at 0.2 V, and the observed bands in this spectrum could be assigned to the vibrational modes of CH_3CN and PPh_3. Therefore, the detected Raman signal in fact comes mainly from the bulk solvent rather than from the surface species. The great differences in the spectral features in this potential region might be caused by the differences in the compositions of the surface films on the surface, that is, the PPh_3 might play an important role in the formation of the surface film and it may modify the properties of the surface complex.

The Role of PPh_3 in the Surface Coordination Chemistry of BTAH

It is well known that PPh_3 serves as a common ligand in metal coordination chemistry. On the basis of the hard–soft acid–base theory, low-valent metal ions (e.g. Cu^+) are a class of soft Lewis acids, whereas PPh_3 is a typical soft base.[57] Therefore, stabilization of the low-valent Cu^+ metal

ion was increased by the interaction of PPh_3 with the metal ion, which resulted in an increase in the softness by increasing the electron density on the metal ion. Generally, more than one PPh_3 molecule coordinated with one Cu^+ ion to form a $Cu(PPh_3)_n^+$ cation.[58–60] Therefore, this cation is a soft acceptor ion that can accommodate a wide range of coordination anions to form air-stable complexes.[61] In the direct electrochemical synthesis, the electrochemical efficiency E_f value of ca. 1.0 mol F^{-1} for both cases indicated that the Cu metal was oxidized to the Cu^+ ion in the electrochemical reaction. As a consequence, the central metal ion was Cu^+, which was quickly stabilized by the soft neutral PPh_3 ligand. Following that, the BTA^- anion that was generated at the cathode participated to form a stable complex. In the final product, the separation of crystalline $Cu(PPh_3)_3Cl$ indicated the formation of $Cu(PPh_3)_3^+$ (Figure 4). However, the structure of the final product in the latter case of $Cu_5Cl(BTA)_5(PPh_3)_4$ indicated that the central Cu^{II} was coordinated to four equatorial and one axial BTA^- ligands to form a distorted tetragonal pyramidal coordination polyhedron, whereas each surrounding Cu^I ion was in a distorted tetrahedral environment and coordinated with one PPh_3 ligand. It revealed that one Cu^I ion was oxidized to Cu^{II} after the electrochemical reaction, and some of the PPh_3 ligands that were coordinated to Cu^I in the initial stage of the electrochemical procedure were exchanged by BTA^- ligands in solution. The proposed surface coordination chemistry of BTAH is presented in Equation (6).

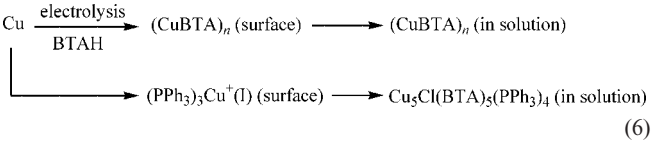

(6)

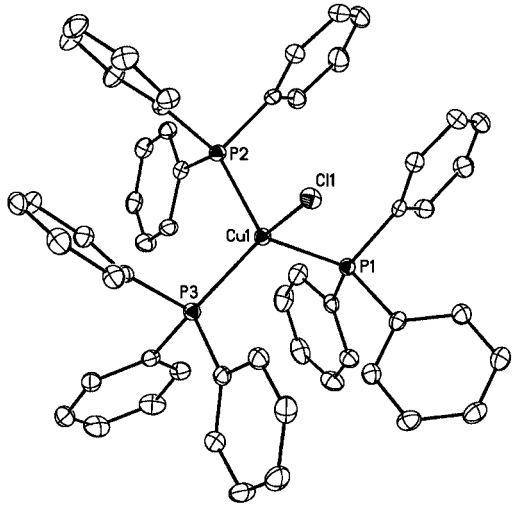

Figure 4. ORTEP drawing of the $Cu_3Cl(PPh_3)_3$ complex. Hydrogen atoms are omitted for clarity.

The in situ SERS measurements were in agreement with the processes of electrochemical synthesis, namely, the soluble $Cu(PPh_3)_3^+$ cation was firstly formed on the surface and then the complex was secondly formed in solution. Thus, the fact that no BTAH film covered the electrode surface resulted in the absence of an SERS signal at +0.2 V. There are two effects that can be attributed to the disappearance of the surface Raman signal of BTAH/BTA^- at +0.2 V: (1) no compact film was formed on the electrode surface and (2) the decrease in the SERS activity because of the dissolution of Cu to form the $Cu(PPh_3)_3^+$ layer in the specific potential region. When the potential was increased again to the severe oxidization region, the surface atoms of the electrode were oxidized to Cu^{2+} which were located at the borderline between being a hard acid and a soft acid. Conversely, because of the increase in the valence of Cu, an increase in the coordination numbers produces steric hindrance that hinders the participation of a large ligand such as PPh_3 in the coordination process. Therefore, the observation of the SERS signal from the BTA^- ion and the absence of the SERS signal from the PPh_3 ligand in the potential region of 0.4 to 0.6 V revealed that the Cu^{2+} ion could be coordinated by the BTA^- anion directly to form a film on the surface again. At +0.6 V, a broad band at ca. 560 cm^{-1} was detected, which was similar to that obtained in the solution without PPh_3. Therefore, it is reasonable to assume that the BTA^- anion showed a similar adsorption or coordination behavior in the most positive potential region, specifically, the formation of surface complex film together with the Cu oxide.

The formation of longchains of the insoluble polymer $[Cu(BTA)]_n$ is suppressed because the neutral PPh_3 ligand participates in the formation of the complex and shows a strong stabilization effect on the complexes. As a consequence, the cation of $Cu(PPh_3)_3^+$ dissolves into CH_3CN quickly and hence no strong signal of BTAH from the surface could be detected in a specific potential region. In fact, it accelerates the dissolution of the Cu electrode rather than strengthening the inhibition efficiency in that potential region; explicitly, the existence of PPh_3 plays a negative role in the inhibition of BTAH at the Cu surface.

Conclusions

The surface coordination of BTAH onto the Cu surface was deduced to involve chemically adsorbed layers, a BTA^- polymer film, and PPh_3-assisted surface dissolution. BTAH exhibits different adsorbed and filmed behaviors in different potential regions in solution. In the extremely negative potential region, the neutral BTAH molecules were adsorbed onto the Cu surface in acetonitrile solutions with or without PPh_3. BTAH also formed an attached polymer film on the surface in the medium without PPh_3, whereas a crystalline complex formed in solutions containing PPh_3. Our preliminary experiment showed that electrochemical synthesis combined with SERS studies could provide the surface coordination mechanism at the molecular level.

Experimental Section

Physical Measurements: BTAH and PPh_3 (Aldrich) were used as received. Solvents were purified by standard methods. C and H

elemental analysis was performed with an Italy Carlo Erba MOD-1106 microanalysis instrument. Raman spectra were measured with a micro-Raman system of LabRam I with a low power He–Ne laser source.

Electrochemical Synthesis of $(CuBTA)_n$, $Cu_5Cl(BTA)_5(PPh_3)_4$: The electrosynthesis of the metal complex was carried out in acetonitrile by using Pt as the cathode and Cu as a sacrificial anode according to the technique described in our previous work.[21] The BTAH ligand (0.2374 g), with or without PPh_3 (0.5230 g), was dissolved in CH_3CN (30 mL) containing a small amount of Et_4NClO_4 as the supporting electrolyte. The electrodes were treated with HNO_3, and washed and dried before use. All operations were carried out under the protection of dry Ar with rigorous exclusion of air by using standard vacuum line techniques. The voltage was regulated to obtain an initial current of 20 mA. As soon as the current flowed in the cell, bubbles of hydrogen gas were visible at the cathode. Five minutes later, pale yellow solids precipitated around the anode piece. After two hours of electrolysis, the Cu piece was rinsed, dried, and weighed to determine the electrochemical efficiency (E_f). A black powder was obtained in the solution without PPh_3 and defined as complex 1. For the system with PPh_3, the solid was isolated by filtration, and then dissolved in a mixture of acetonitrile/chloroform (1:1; complex 2). One week later, brown crystals of $Cu_5(BTA)_5(PPh_3)_4Cl{\cdot}2CH_3CN$ were separated out from the solution in a yield of ca. 63%. A little quantity of $Cu(PPh_3)_3Cl$ was separated from the final product and its structure was determined.

X-ray Structure Determination: $C_{106}H_{86}ClCu_5N_{17}P_4$ (2075.04): calcd. C 61.35, H 4.18, N 11.47; found C 59.74, H 4.15, N 10.55. A brown crystal having approximate dimensions of $0.60 \times 0.36 \times 0.35$ mm was selected and mounted on a glass fiber. All measurements were made with a Rigaku Mercury CCD diffractometer equipped with graphite-monochromated Mo-K_α (λ = 0.71070 Å) radiation by using an ω scan mode in the range $3.02 < \theta < 27.48°$ at 193(2) K. A total of 99572 reflections were collected, of which 17353 with $I > 2\sigma(I)$ out of 21901 were unique ones (R_{int} = 0.0512) were considered as observed. All of the calculations were performed by using the SHELXS-97package.[62] The structure was solved by direct methods and refined by full-matrix least-squares techniques on F^2. All non-hydrogen atoms were refined anisotropically, whereas the hydrogen atoms included in the final cycle of refinement were located on the calculated positions boned to their carrier atoms. The weighting scheme was $w = 1/[\sigma^2(F_o^2) + (0.0739P)^2 + 24.2198P]$, where $P = (F_o^2 + 2F_c^2)/3$, S = 1.069. The final R indices R_1 = 0.0704, wR_2 = 0.1643[$I > 2\sigma(I)$]. The crystallographic data is summarized in Table 2, and the crystal structure is presented in Figure 2. CCDC-283457 contains the supplementary crystallographic data for this paper. These data can be obtained free of charge from The Cambridge Crystallographic Data Centre via www.ccdc.cam.ac.uk/data_request/cif.

The In Situ Electrochemical SERS Measurements: Raman spectra were recorded with a confocal micro-Raman system (LabRam I from Dilor). The microscope attachment was based on an Olympus BX40 system and used a 50× long working length objective (≈ 8 mm) so that the objective would not be immersed into the solution. All the experiments were performed with the excitation line of 632.8 nm from an internal He–Ne laser with a power of 4 mW on the electrode surface. The electrochemical cell for the SERS measurement was made by Teflon with a quartz window for introducing the laser and collecting the Raman signal. The working electrode was a Cu disk with a geometric area of 0.1 cm^2 embedded in a Teflon rod. It was polished successively with 1 and 0.05 μm alumina powder and sonicated in triply distilled water. Consequently, a double potential step from –0.4 to + 0.4 V (vs. SCE) was applied to the electrode in 0.1 M KCl solution for about 2 min followed by a potential excursion at –0.4 V for 1 min, and then, it was rinsed thoroughly and dried with nitrogen to remove traces of water on the surface. A large Pt ring served as the counter electrode. The reference electrode was a solid Ag/AgCl electrode, which was prepared by electrochemical oxidation of an Ag wire with a constant anodic current of 0.4 $mA\,cm^{-2}$ in a 0.1 M HCl solution for 30 min. A detailed description of the spectroelectrochemical measurements is given elsewhere.[9,40] All experiments were performed at room temperature. All the chemicals used were analytical reagent grade. The solutions were prepared by using acetonitrile, which was pretreated to remove water.

Table 2. Crystal data for $Cu_5(BTA)_5(PPh_3)_4Cl{\cdot}2CH_3CN$.

Empirical formula	$C_{106}H_{86}ClCu_5N_{17}P_4$
Formula weight	2074.95
Crystal system	monoclinic
Space group	$P2_1/n$
a [Å]	16.739(2)
b [Å]	18.919(2)
c [Å]	31.042(4)
β [°]	103.194(3)
V [$Å^3$]	9571.0(19)
Z value	4
Crystal dimensions [mm]	$0.60 \times 0.36 \times 0.35$
$D_{calcd.}$ [$g\,cm^{-3}$]	1.440
$F(000)$	4252
Total reflections measured	99572
Unique	21901
Residuals: R_1 [$I > 2\sigma(I)$]	0.0704
Residuals: wR_2 [$I > 2\sigma(I)$]	0.1643
Maximum peak in final diff. map [$e\,Å^3$]	1.764
Minimum peak in final diff. map [$e\,Å^3$]	–1.382

Acknowledgments

The authors gratefully acknowledge the financial support from the Nature Science Foundation of China (20503019, 20573076) and the Natural Science Foundation of Jiangsu Province (BK2005032). Y. X. Y. is partially supported by the Key Academic Discipline of Organic Chemistry of Jiangsu Province and Suzhou University for Young Teachers.

[1] J. Handley, D. Collison, C. D. Garner, M. Helliwell, R. Docherty, J. R. Lawson, P. A. Tasker, *Angew. Chem. Int. Ed. Engl.* **1993**, *32*, 1036–1038.
[2] M. Frey, S. G. Haris, J. M. Holmes, D. A. Nation, S. Parsons, P. A. Tasker, S. J. Teat, R. E. P. Winpenny, *Angew. Chem. Int. Ed.* **1998**, *37*, 2193–2197.
[3] J. M. Thorpe, R. L. Beddoes, D. Collison, C. D. Garner, M. Helliwell, J. M. Holmes, P. A. Tasker, *Angew. Chem. Int. Ed.* **1999**, *38*, 1119–1121.
[4] M. P. Soriaga, *Chem. Rev.* **1990**, *90*, 771–793.
[5] C. A. Melendres, N. Camillone, T. Tipton, *Electrochim. Acta* **1989**, *34*, 281–286.
[6] I. Dugdale, J. B. Cotton, *Corros. Sci.* **1963**, *3*, 69–74.
[7] R. Walker, R. C. Benn, *Electrochim. Acta* **1971**, *16*, 1081–1088.
[8] G. Xue, J. F. Ding, P. Lu, J. Dong, *J. Phys. Chem.* **1991**, *95*, 7380–7384.
[9] J. L. Yao, Y. X. Yuan, R. A. Gu, *J. Electroanal. Chem.* **2004**, *573*, 255–261.
[10] D. Chadwick, T. Hashemi, *Corros. Sci.* **1978**, *18*, 39–51.
[11] J. O'M. Bockris, M. A. Habib, J. L. Carbajal, *J. Electrochem. Soc.* **1984**, *131*, 3032–3033.

[12] J. Rubim, I. G. R. Gutz, O. Sala, W. J. Orvillethomas, *J. Mol. Struct.* **1983**, *100*, 571–583.
[13] J. P. Lang, X. Q. Xin, *J. Solid State Chem.* **1994**,*108*, 118–127.
[14] T. A. Annan, D. G. Tuck, *Organometallics* **1991**, *10*, 2159–2166.
[15] C. Oldham, M. J. Taylor, D. G. Tuck, *Inorg. Chim. Acta* **1985**, *100*, L9–L10.
[16] R. Castro, J. Romero, J. A. Garcia-Vazquez, M. L. Duran, A. Castineiras, A. Sousa, *J. Chem. Soc. Dalton Trans.* **1990**, 3255–3258.
[17] M. L. Duran, J. Romero, J. A. Garcia-Vazquez, R. Castro, A. Castineiras, A. Sousa, *Polyhedron* **1991**, *10*, 197–202.
[18] R. Castro, M. L. Duran, J. A. Garcia-Vazquez, J. Romero, A. Sousa, A. Castineiras, W. Hiller, J. Strahle, *J. Chem. Soc. Dalton Trans.* **1990**, 531–534.
[19] T. A. Annan, J. Gu, Z. Tian, D. G. Tuck, *J. Chem. Soc. Dalton Trans.* **1992**, 3061–3067.
[20] W. Y. Vivian, W. K. Lee, T. F. Lai, *Organometallics* **1993**, *12*, 2383–2387.
[21] Y. Yuan, J. Yao, J. Lu, Y. Zhang, R. Gu, *Inorg. Chem. Commun.* **2005**, *8*, 1014–1017.
[22] Y. Yamamoto, H. Nishihara, K. Aramaki, *Corrosion* **1992**, *48*, 641–648.
[23] L. J. Wan, *Acc. Chem. Res.* **2006**, *39*, 334–342.
[24] S. J. Huo, Q. X. Li, Y. G. Yan, Y. Chen, W. B. Cai, Q. J. Xu, M. Osawa, *J. Phys. Chem. B* **2005**, *109*, 15985–15991.
[25] Y. G. Yan, S. J. Huo, Q. J. Xu, W. B. Cai, *J. Phys. Chem. B* **2006**, *110*, 14911–14915.
[26] Z. Q. Tian, B. Ren, "Infrared and Raman Spectroscopy in Analysis of Surfaces" in *Encyclopedia of Analytical Chemistry* (Ed.: R. A. Meyers), John Wiley & Sons, Chichester, **2000**, pp. 9162–9201.
[27] K. Kneipp, H. Kneipp, I. Itzkan, R. R. Dasari, M. S. Feld, *Chem. Rev.* **1999**, *99*, 2957–2975.
[28] B. Pettinger in *Adsorption at Electrode Surface* (Eds.: J. Lipkowski, P. N. Ross), VCH, New York, **1992**, pp. 285–345.
[29] L. W. H. Leung, M. J. Weaver, *J. Electroanal. Chem.* **1987**, *217*, 367–384.
[30] Y. Zhang, X. Gao, M. J. Weaver, *J. Phys. Chem.* **1993**, *97*, 8656–8663.
[31] M. Fleischmann, Z. Q. Tian, L. J. Li, *J. Electroanal. Chem.* **1987**, *217*, 397–410.
[32] B. Pettinger, H. Wetzel, "Organic and Inorganic Species at Ag, Cu, and Au Electrodes" in *Surface Enhanced Raman Scattering* (Eds.: R. K. Chang, T. E. Furtak), Plenum, New York, USA, **1982**, pp. 293–314.
[33] R. K. Chang, "Raman Spectroscopic Techniques in Interfacial Electrochemistry" in *Spectroscopic and Diffraction Techniques in Interfacial Electrochemistry* (Eds.: C. Gutierrez, C. Melendres), Kluwer Academic, Drodrecht, Netherlands, **1990**, pp. 155–180.
[34] J. Lipkowski, L. Stolberg, "Molecular Adsorption at Gold and Silver Electrodes" in *Adsorption of Molecules at Metal Electrodes* (Eds.: J. Lipkowski, P. N. Ross), VCH, New York, USA, **1992**, ch. 4, pp. 171–238.
[35] J. B. Cotton, I. R. Scholes, *Br. Corros. J.* **1967**, *2*, 1–5.
[36] R. Youda, H. Nishihara, K. Aramaki, *Corros. Sci.* **1988**, *28*, 87–96.
[37] J. Kester, T. Furtak, *J. Electrochem. Soc.* **1981**, *128*, 112–112.
[38] P. G. Cao, J. L. Yao, J. W. Zheng, R. A. Gu, Z. Q. Tian, *Langmuir* **2002**, *18*, 100–104.
[39] P. G. Cao, R. A. Gu, Z. Q. Tian, *Langmuir* **2002**, *18*, 7609–7615.
[40] R. F. V. Villamil, P. Corio, J. C. Rubim, S. M. L. Agostinho, *J. Electroanal. Chem.* **1999**, *472*, 112–120.
[41] M. Fleischmann, I. R. Hill, G. Mengoli, M. M. Musiani, *Electrochim. Acta* **1983**, *28*, 1325–1333.
[42] Y. C. Wu, P. Zhang, H. W. Pickering, D. L. Allara, *J. Electrochem. Soc.* **1993**, *140*, 2791–2800.
[43] J. L. Yao, B. Ren, Z. F. Huang, P. G. Cao, R. A. Gu, Z. Q. Tian, *Electrochim. Acta* **2003**, *48*, 1263–1271.
[44] V. L. Himes, *J. Am. Chem. Soc.* **1981**, *103*, 211–212.
[45] E. G. Bakalbassis, E. Diamantopoulou, S. P. Perlepes, C. P. Raptopoulou, V. Tangoulis, A. Terzis, T. F. Zafiropoulous, *J. Chem. Soc. Chem. Commun.* **1995**, 1347–1348.
[46] E. Diamantopoulou, C. P. Raptopoulou, A. Terzis, V. Tangoulis, S. P. Perlepes, *Polyhedron* **2002**, *21*, 2117–2126.
[47] M. Murrie, D. Collison, C. Garner, M. Helliwell, P. A. Tasker, S. S. Turner, *Polyhedron* **1998**, *17*, 3031–3043.
[48] D. Collison, E. J. L. McInnes, E. K. Brechin, *Eur. J. Inorg. Chem.* **2006**, 2725–2733.
[49] D. Li, R. Li, Z. Qi, X. Feng, J. Cai, X. Shi, *Inorg. Chem. Commun.* **2001**, *4*, 483–485.
[50] G. Kickelbick, H. J. Paik, K. Matyjaszewski, *Macromolecules* **1999**, *32*, 2941–2947.
[51] I. Fenger, C. Le Drian, *Tetrahedron Lett.* **1998**, *39*, 4287–4291.
[52] K. Dehnicke, F. Weller, *Coord. Chem. Rev.* **1997**, *158*, 103–169.
[53] K. Nomiya, R. Noguchi, M. Oda, *Inorg. Chim. Acta* **2000**, *298*, 24–32.
[54] R. Pikl, F. Duschek, C. Fickert, R. Finsterer, W. Kiefer, *Vib. Spectrosc.* **1997**, *14*, 189–197.
[55] R. T. Jonas, T. D. P. Stack, *Inorg. Chem.* **1998**, *37*, 6615–6629.
[56] T. Kräuter, B. Neumüller, *Polyhedron* **1996**, *15*, 2851–2857.
[57] R. G. Pearson, *J. Am. Chem. Soc.* **1963**, *85*, 3533–3539.
[58] P. F. Barron, J. C. Dyason, P. C. Healy, L. M. Engelhardt, C. J. Pakawatchai, *J. Chem. Soc. Dalton Trans.* **1987**, 1099–1106.
[59] D. J. Fife, W. M. Moore, K. W. Morse, *Inorg. Chem.* **1984**, *23*, 1684–1691.
[60] G. Doyle, K. A. Eriksen, D. V. Engen, *Organometallics* **1985**, *4*, 830–835.
[61] R. D. Hart, P. C. Healy, G. A. Hope, D. W. Turner, A. H. White, *J. Chem. Soc. Dalton Trans.* **1994**, 773–779.
[62] G. M. Sheldrick, *SHELX-97 and SHELXL-97: Program for Crystal Structure Refinement*, University of Göttingen, Germany, **1997**.

Received: April 20, 2007
Published Online: September 10, 2007

